The Fourth International Symposium on Innovative Nuclear Energy Systems INES-4

Criticality uncertainty dependence on nuclear data library in Fast Molten Salt Reactors

W.F.G. van Rooijen*, Y. Shimazu, N. Yamano

Research Institute of Nuclear Engineering, University of Fukui, Kannawa-cho 1-2-4, Tsuruga-shi, Fukui-ken, 914-0055, Japan

Abstract

To increase the sustainability of the nuclear fuel cycle, and increase security of nuclear energy, we have been investigating Molten Salt Fast Reactors (MSFR) for transmutation of Minor actinoid (MA) isotopes. In the present work we describe the reactor physics analysis of a Th-TRU MSFR using a LiF-ThF_4-$TRUF_3$-fuel salt. We investigated the uncertainty of major reactor physics parameters using 3 sets of evaluated nuclear data: JENDL-4.0, JEFF-3.1.2, and ENDF/B-VII.1. The result of our work is that the spread in the multiplication factor is rather large between the sets of nuclear data, while other parameters are by and large the same. The uncertainties due to cross section covariance are large, with Th-232, U-233, and F-19 giving the most important contributions. The isotopic contributions to the uncertainties are quite different between the sets of nuclear data, giving a suspicion that the covariance data may is very different between the evaluations, and a review of the covariance data may be needed.

Keywords: Nuclear Transmutation, Molten Salt Reactor, Nuclear Data, Uncertainty Analysis, Cross Section Processing.

1. Introduction

For the long-term sustainability of the nuclear fuel cycle, and to increase security of nuclear power as a source of energy, it is important to address the issue of long-lived nuclear waste (HLW, High Level Waste). In the present paper we investigate a Molten Salt Reactor for MA transmutation: Molten Salt Fast Reactor (MSFR). The reactor uses a thorium-TRU (TRans-Uranium) fuel. The Molten Salt Reactor concept offers several attractive features for transmutation of Minor actinoid (MA) isotopes: online refueling and reprocessing, negative reactivity coefficients for fuel temperature and density, and the potential to discharge the fuel to a safe container in case of a severe accident. In the present work, reactor phsyical parameters (reactivity, Doppler coefficient, fuel density coefficient, delayed neutron fraction) are calculated and their uncertainties, using three modern sets of evaluated nuclear data: JENDL-4.0, JEFF-3.1.2, and ENDF/B-VII.1. The result is that all three of these sets of nuclear data require improvements for application to MSFR.

---
*Corresponding author
Email address: rooijen@u-fukui.ac.jp (W.F.G. van Rooijen)
URL: http://www.rine.u-fukui.ac.jp/ (W.F.G. van Rooijen)

2. Fuel salt composition

For the present work, we focus on a fluoride molten salt. While there is much information about salt compositions for tetravalent fluoride compounds (ThF_4 and UF_4), there is much fewer information about the trivalent fluoride compounds (PuF_3, AmF_3, etc). After literature review [1, 2, 3, 4]), we decided on the following salt compostion: $LiF-ThF_4-TRUF_3$ (78/17/5 mole%, TRU = TRans Uranium isotopes). In Figure 1 is given phase diagram of this fuel salt. From Figure 1 it is seen that the chosen composition is near the eutectic point, and the melting point was estimated as 850 K. The density was estimated as $\rho(T) = 5.54 - 1.25 \times 10^{-3}T$ g cm^{-3}, with T the temperature in Kelvin [5].
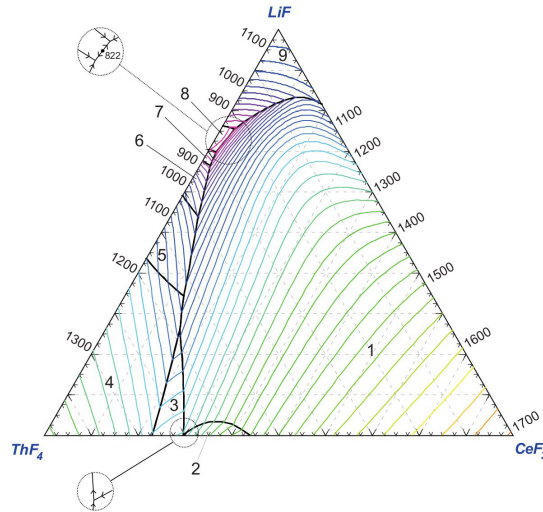

Fig. 1. Phase diagram of the $LiF-ThF_4-CeF_3$-system, taken from [3]. CeF_3 is an analogon for PuF_3, and in the present work it is assumed that Np, Am, and Cm have similar behavior. From this diagram it is clear that addition of PuF_3 to the fuel salt rapidly increases the melting point. The composition for the present work, $LiF-ThF_4-TRUF_3$ at 78/17/5 mole%, is in the upper right hand corner of the upper circle.

A representative core composition was derived from the following considerations: to maintain the melting point of the fuel salt, the fraction of TRU should be constant, as should the fraction of Th + U (the chemical behavior of ThF_4 is similar to UF_4 [4]). Also, the concentration of fission products in the fuel salt should remain low. During operation, Th and TRU are continuously added to the reactor. The fissile isotopes in the TRU will deplete very quickly. Therefore, sustained operation is possible if the production of U-233 from Th-232 balances the reactivity loss of the TRU material. The equilibrium ratio of U-233 to Th-232 is given by $N_{23}/N_{02} \approx \sigma_{c,02}/\sigma_{c,23} \approx 0.14$, where index "02" indicates Th-232 and "23" indicates U-233. Thus, to maintain the salt composition in an acceptable range, the rate of addition of TRU should be the same as the rate of consumption; to maintain the fraction of Th + U, one adds Th at a sufficient rate, and any surplus U-233 is to be continuously removed (note: as long as the "enrichment" in U-233 is below the equilibrium value, there will be an overproduction of U-233).

3. Scoping calculations for the fuel cycle

In the present work, we have assumed that the TRU originates from recycled BWR-MOX fuel. The TRU composition was calculated assuming an ABWR-type reactor (specifically, the ABWR under construction in Oma, Japan), with a full MOX core. The fuel is irradiated to 55000 GWd/t, and subsequently a cooling period of 15 year is assumed. At present, further details, such as shuffling patterns and/or fuel batching are not taken into account. The core-averaged composition of the TRU is given in Table 1. The basic mode of

operation is as follows: while the reactor is running, a combination of Th-232, U-233 and TRU is added to, or extracted from to the reactor as required to maintain criticality, and to maintain the fuel salt composition. Given that the TRU vector and the fraction of TRU in the fuel salt are known (from the requirement on the fuel melting point), one needs to determine the rate of TRU addition to the reactor, the U-233 enrichment for criticality, the rate of Th addition, the rate of U reprocessing, and the rate of reprocessing for the fission products, so that the reactor remain critical and the fractions of Th, U, and TRU are constant in the fuel. Calculations were done assuming 10 years of continuous operation with a continuous feed of thorium and TRU, and a continuous reprocessing of U-233 and fission products. It is assumed that initially a sufficient supply of U-233 is available to start the reactor (for example, from a dedicated U-233 production reactor or from irradiation of Th-232 fuel in LWRs).

Table 1. TRU composition.

Isotope	Weight%	Mole%	Isotope	Weight%	Mole%
Np-237	0.352 53	0.354 51	Am-241	4.8943	4.8399
Np	0.3525	0.3545	Am-243	2.1885	2.1463
Pu-238	2.3980	2.4013	**Am**	7.113	7.016
Pu-239	35.001	34.902	Cm-244	0.829 35	0.810 03
Pu-240	32.390	32.164	Cm-245	0.745 03	0.724 70
Pu-241	12.372	12.235	**Cm**	1.584	1.545
Pu-242	9.5280	9.3831			
Pu	91.69	91.09			

Calculations were done with the SCALE-6 code system [6], specifically the TRITON module to generate effective cross sections for the depletion calculations, and ORIGEN-S for the depletion calculations. All calculations are done based on the SCALE-6 238-group ENDF/B-VII.1 cross section library. ORIGEN-S has options to take into account both a continuous feed (MFEED option) and continuous reprocessing (MPROS option). Continuous reprocessing is simulated by adding a "chemical removal constant" λ_c, i.e. for isotope i the disappearance term becomes $\sigma_{a,i}\phi + \lambda_i + \lambda_{c,i}$. λ_c is the same for all isotopes of a given chemical element. Several "reprocessing groups" were defined, each with a different chemical removal constant, as given in Table 2. For example, it is assumed that all noble gases will be removed with a very short time constant from the fuel salt. For the time being, it is assumed that basically all fission products are removed with the same removal constant. Obviously, the validity of these assumptions will need to be investigated more deeply in the future.

Table 2. Addition and removal rates for continuous refueling and reprocessing in the MSFR. "Period" indicates the period in the periodic table, i.e. period n is the nth row in the periodic table.

Addition rates [mole.s^{-1}]		Removal constants [s^{-1}]	
Th	4.5×10^{-6}	Noble gases (He, Kr, Xe)	1.0×10^{-3}
TRU	3.3×10^{-6}	Period 5 Fission Products (Y to I)	1.0×10^{-4}
		Period 6 Fission Products (Lanthanoids)	1.0×10^{-5}
		H, N, O	2.0×10^{-4}
		Uranium	6.0×10^{-9}

ORIGEN-S can calculate the k_∞ of the depletion mixture, based on the 1-group depletion cross sections. This k_∞ is not very accurate, but good enough for scoping calculations. With the settings of Table 2, the k_∞

of Figure 2(a) was found for the first ten years of operation. Since $k_\infty \approx 1.10$ there is sufficient margin for the finite size of the system. In Figure 2(b) is given the salt composition during 10 years of operation.
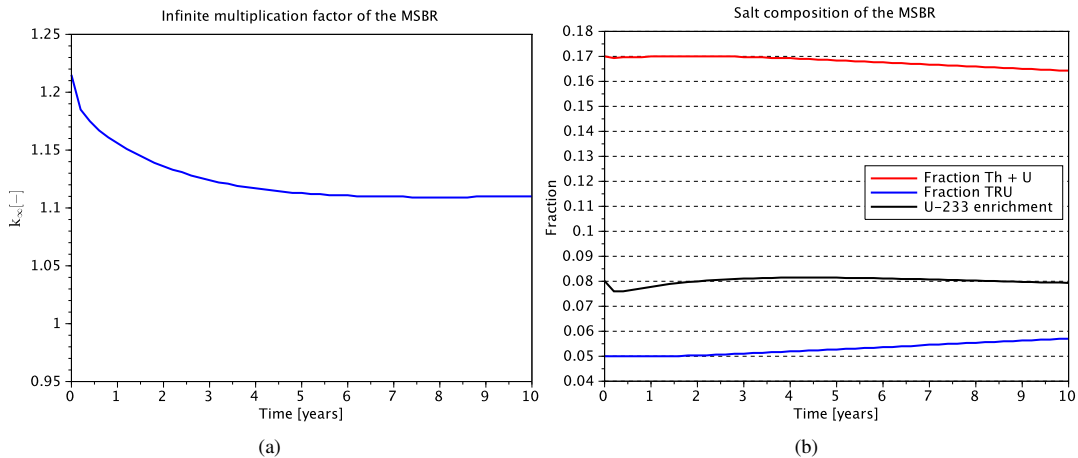

Fig. 2. 2(a): k_∞ during 10 years of operation of the Th-TRU MSBR. 2(b): salt composition of the MSBR. As can be seen, the fraction of TRU increases towards the end of the irradiation, which may be problematic. However, given the uncertainties related to the chemistry of the salt, we think that the present result is adequate for a scoping study.

4. MSBR cross section uncertainty analysis

Based on the results of the fuel cycle calculation of the MSBR, the fuel composition at 6 years of operation was taken as a reference composition for a more detailed analysis of the reactor physical properties. Note here that depletion calculations are only performed with the ENDF/B-VII.1 cross sections of SCALE6, in other words, there is only one composition at 6 years; the corresponding reactor physical properties are analyzed with 3 different sets of nuclear data. The reactor core of the MSBR is homogeneous (it is a fast reactor, there is no moderator), and cylindrical with a radius $R = 0.9$ m and a height $H = 1.85$ m, for a volume of about 4.7 m^3. Reactor power is chosen as 1400 MWth, which corresponds to around 300 MW m^{-3}. The composition of the fuel salt is given in Table 3.

Analysis is done with the fast reactor analysis code ERANOS-2.0 code [7], using transport theory (SN-calculations) in RZ-geometry. At the University of Fukui we have created a cross section processing tool to make cross section libraries for ECCO, which is the cell code in ERANOS. One of the notable features of ECCO is that it uses more than one energy group structure. For the present work, calculations are performed in 1968 groups for the so-called *major isotopes* (actinoids), and in 33 groups for so-called *minor isotopes*. For reference, the process of creating cross sections for ECCO is briefly indicated here (see also Figure 3):

- For each isotope, the first step is to use NJOY to create a group-wise cross section library in 1968 groups.
- For each isotope, CALENDF is used to generate probability tables, used in the sub-group calculation in ECCO.
- The MERGE code merges together the cross section libraries from NJOY and CALENDF.
- The code GECCO translates the library into the ECCO format.
- ERANOS is used to merge the libraries of individual isotopes together.

Table 3. The composition of the fuel salt after 6 years of continuous operation, with continuous refueling and reprocessing. Note: for brevity, only important isotopes are given.

Isotope	Atomic density [at/b.cm]	Fraction in HM [%]	Isotope	Atomic density [at/b.cm]	Fraction in HM [%]
Li-7	2.340×10^{-2}		Am-241	4.719×10^{-5}	0.74
F-19	4.812×10^{-2}		Am-242	3.841×10^{-8}	0.00
Th-232	4.430×10^{-3}	69.33	Am-242m	5.158×10^{-6}	0.08
U-233	4.297×10^{-4}	6.72	Am-243	5.947×10^{-5}	0.93
U-234	8.316×10^{-5}	1.30	Cm-242	7.562×10^{-6}	0.12
U-235	1.043×10^{-5}	0.16	Cm-243	1.034×10^{-6}	0.02
Np-237	2.725×10^{-6}	0.04	Cm-244	5.405×10^{-5}	0.85
Pu-238	5.421×10^{-5}	0.85	Cm-245	1.320×10^{-5}	0.21
Pu-239	2.368×10^{-4}	3.71	Cm-246	1.907×10^{-6}	0.03
Pu-240	6.009×10^{-4}	9.40			
Pu-241	1.478×10^{-4}	2.31			
Pu-242	2.079×10^{-4}	3.25			

- ERANOS (ECCO) is used to generate a weighting spectrum, and the 1968 group library is collapsed to 33 groups.

- Finally, one has two ECCO libraries, one in 1968 groups and one with 33 groups. For *major* isotopes, both the 1968-group and 33-group libraries are retained; for *minor* isotopes, the 1968-group library is discarded and only the 33-group library is maintained.

- The ERRORR module of NJOY is used to generate covariance data in 33 groups for each isotope for which covariance data is available.

- Finally, the ERRORR libraries are re-formatted for use in ERANOS in the so-called AMERE format, and the covariance data is assembled into one file for all isotopes.

The performance of this cross section processing system has been described in other publications [8, 9]. In the present research, we have compared three sets of evaluated nuclear data: JENDL-4.0, JEFF-3.1.2, and ENDF/B-VII.1. The result for the major reactor physics parameters is given in Table 4:

- The reactivity is given, defined as $\rho = (k - 1)/k$ where k is the effective multiplication factor.[1]

- The Doppler coefficient is calculated by increasing the temperature of isotopes in the fuel salt by 200 K; the Doppler coefficient is calculated as $\alpha_D = (\rho(T_1) - \rho(T_0))/\Delta T$. The Doppler coefficient takes into account the change of the cross sections only, i.e., thermal expansion is not taken into account.

- The fuel density coefficient (also referred to as "void coefficient") is calculated by decreasing the fuel density by 1%, simulating the effect of thermal expansion. The coefficient is then simply evaluated as $\rho_1 - \rho_0$ where ρ_0 is the reactivity of the reference state and ρ_1 is the reactivity when the fuel salt density is decreased.

Note here that the spread of the reactivities is rather large, ranging from about 1000 pcm ($k \approx 1.01$) for JENDL-4.0 to about 4000 pcm for ENDF/B-VII.1 ($k \approx 1.04$). The Doppler coefficient and the effective

---

[1]Note: the reactivity ρ is not to be confused with the density $\rho(T)$ introduced earlier in the paper; to avoid confusion, we will use the word "reactivity" from now on and avoid the symbol ρ.
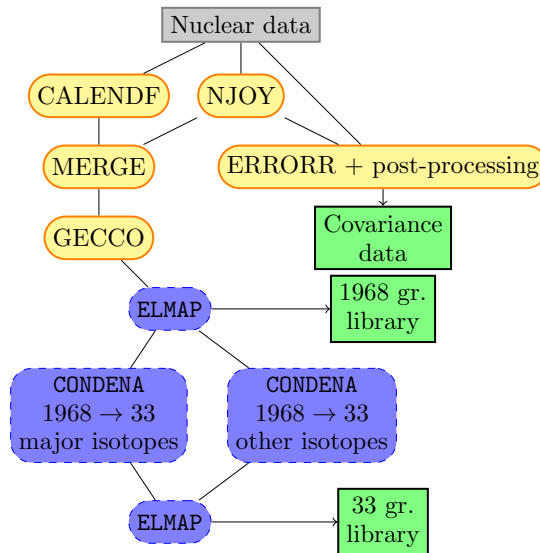
Fig. 3. Flow chart describing the process to generate ECCO libraries and covariance data for ERANOS.

delayed neutron fraction are very much comparable to those in a traditional fast breeder reactor [10]. The uncertainties are relatively large: for the reactivity (related to the multiplication factor), the uncertainty amounts to about 2%, which is about 3 times larger than in the case of Monju (a fast reactor with traditional uranium - plutonium fuel); similarly the uncertainty on the Doppler coefficient is relatively large.

Table 4. Results for the main parameters of interest.

	JENDL 4.0	JEFF 3.1.2	ENDF/B VII.1
Reactivity [pcm]	1133	2834	4317
Uncertainty [%]	2.28	2.04	2.08
β [pcm]	314	315	311
Doppler [pcm/K]	-2.19	-1.87	-2.29
Uncertainty [%]	7.54	5.64	4.94
Density [pcm/%]	-140	-145	-151
Uncertainty [%]	0.92	2.51	1.46

In the present study we aim to compare the performance of three sets of evaluated nuclear data. In reality, each set of evaluated nuclear data is based on a specific selection of measured data as well as theoretical modeling. In the optimal case the three sets of data should be completely independent but in reality that is not the case. However, it is expected that if data set A has $\sigma_x = A \pm \delta A$, and data set B has $\sigma_x = B \pm \delta B$, then $A \approx B$ and $\delta A \approx \delta B$. If this does not hold, then either data set A or B or both data sets must be revised.

The three sets of evaluated nuclear data give a different reactivity of the reactor. To determine which isotopes and which reaction types are the cause of these differences a perturbation analysis was performed. In this case, the reactivity calculated with JENDL-4.0 is taken as the reference, and for JEFF-3.1.2 and ENDF/B-VII.1 the difference of the reactivity due to individual isotopes and reaction types was calculated. The result is given in Figure 4. In figure 5, the contributions of individual isotopes to the effective delayed

neutron fraction are shown.

Most isotopic contributions are not very surprising (Th-232, U-233, Pu-240, and Pu-241). The contribution of the inelastic scattering reaction on F-19 is surprising. Inelastic scattering is usually a rather minor reaction. However, in the present case it accounts for approximately 2% difference between JENDL-4.0 and the other data sets. Reading the comment section in the ENDF files, it is revealed that the F-19 cross section and covariance data are the same in JEFF-3.1.2 and ENDF/B-VII.1 (JEFF data is taken from ENDF/B-VII). JENDL-4.0 has different cross section data and no covariance data. However, in all three sets of nuclear data, the inelastic cross section of F-19 up to 1 MeV is based on (only) one and the same measurement, which is labeled as "Broder, 1970". The three data sets differ in the way that this measured data is used; in JEFF-3.1.2 and ENDF/B-VII.1, the following is written: "In the energy up 1 MeV F-19 has inelastic channels starting at the energies 109.9 keV with spin 1/2- and 197.2 keV with spin 5/2+. These two channels were included in the Reich-Moore evalaution with SAMMY. At the present time, cross section processing codes do not have capability to include inelastic channels. Therefore, the evaluation presented here is the pointwise cross section processed with SAMMY." In JENDL-4.0, only MF3 (cross sections) is present. In Figure 6 is given the inelastic cross section of F-19. While the cross section is certainly not identical be0tween JENDL-4.0 on the one hand and JEFF-3.1.2 and ENDF/B-VII.1 on the other, the difference is not so big as to expect a large influence on the reactivity. It is therefore hypothesized that the influence on the reactivity is probably due to a different distribution of the out-going energy. This is presently under investigation.
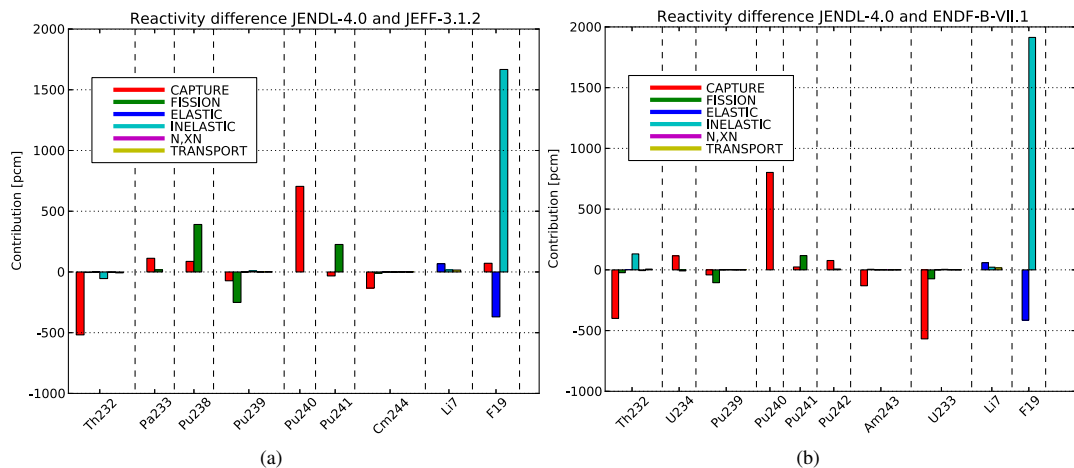

Fig. 4. 4(a): Contributions to the difference of the reactivity between JENDL-4.0 and JEFF-3.1.2. 4(b): Contributions to the difference of the reactivity between JENDL-4.0 and ENDF/B-VII.1.

In Figure 7 is given a breakdown of the isotopic contributions to the uncertainty of the reactivity for each set of evaluated nuclear data. Some points of interest are the large contribution of Th-232 capture in JENDL-4.0 compared to the other nuclear data sets. On the reverse, U-233 gives a small uncertainty in JENDL-4.0 but a large contribution in the other two nuclear data sets. Pu-241 gives a large contribution in JEFF-3.1.2. This is an effect which we also observed in other studies. For JEFF-3.1.2 the covariance data is taken from the BOLNA covariance matrix [11] and apparently this matrix has a relatively large covariance for Pu-241 fission.

In Figure 8 is given a breakdown of the isotopic contributions to the uncertainty of the Doppler coefficient. The Doppler effect is caused by broadening of the capture resonances, hence one expects that the uncertainty of the Doppler coefficient mainly comes from the heavy metal isotopes. ENDF/B-VII.1 is the only evaluated nuclear data set with covariance data for Li-7 and F-19. The contributions of these isotopes is sizeable.

In Figure 9 is given a breakdown of the isotopic contributions to the uncertainty of the fuel density
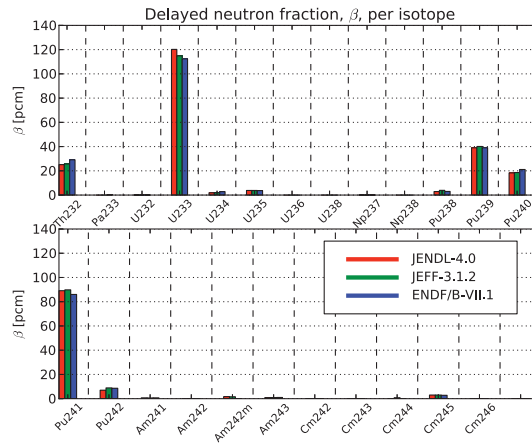
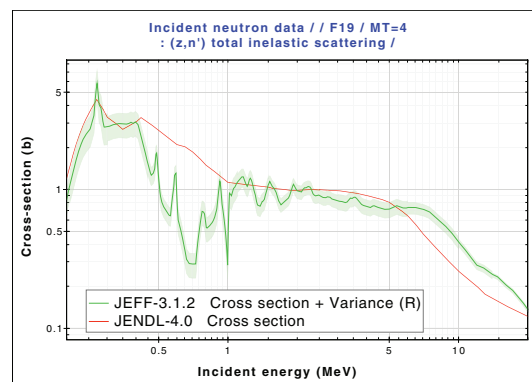Fig. 5. Contributions to the delayed neutron fraction.

Fig. 6. F-19 inelastic cross section for JENDL-4.0 and JEFF-3.1.2 (ENDF/B-VII.1 is same as JEFF-3.1.2) For JEFF-3.1.2 the covariance is also indicated.

coefficient (void coefficient). Here also, the contribution of Th-232 capture in JENDL-4.0 is large, whereas the contribution of U-233 fission is relatively small. In this case, also several isotopes from the stainless steel reflector give a contribution to the uncertainty. This is expected: if the density of the fuel is reduced (even if only slightly), the fuel salt becomes more "transparent" and the result is that the leakage of neutrons to the reflector increases. With more neutrons entering the reflector, the uncertainty due to isotopes in the reflector will have an influence on the overall uncertainty.

5. Discussion & concluding remark

In this paper a preliminary analysis of a Th-MA fueled Molten Salt Fast Reactor has been presented. The presence of trivalent actinoids in the fuel salt (PuF_3, AmF_3, etc) increases the melting pointing of the fuel salt. This is an important problem, because of temperature limits on the reactor components. The $TRUF_3$ loading must remain below a few mole-percent.

As far as the reactor physical parameters is concerned, the spread in reactivity (related to the effective multiplication factor) between JENDL-4.0, JEFF-3.1.2 and ENDF/B-VII.1 is rather large (about 3%). The uncertainty is on the order of 2%, but this is an underestimation, because covariance data for important
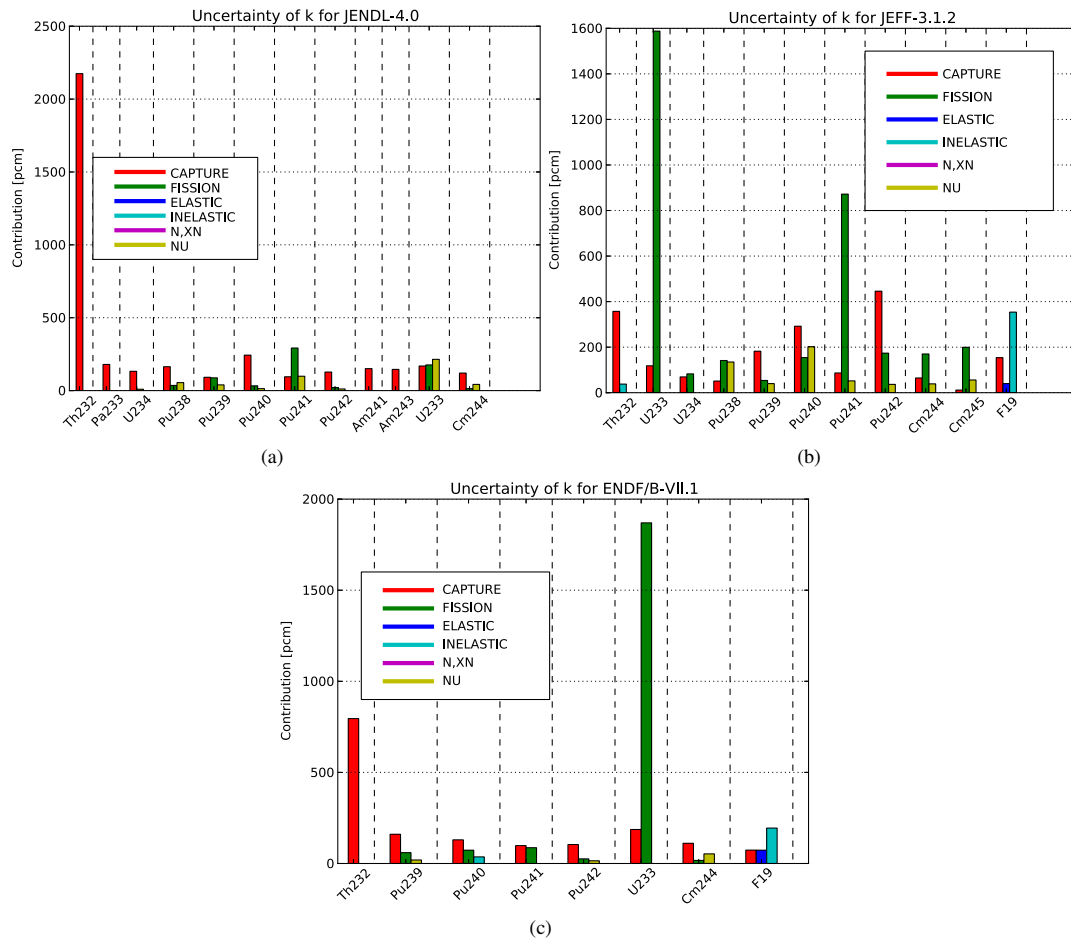
Fig. 7. For each set of nuclear data, the contribution of each isotope to the reactivity (k_{eff}) uncertainty.

isotopes is missing in some cases, notably for F-19 and Li-7 in JENDL-4.0. Another important observation is that while the overall uncertainties are more or less the same for the three sets of nuclear data, the distribution over the isotopes differs considerably. The most notable example is Th-232 capture, which is very important in JENDL-4.0 for the Doppler- and fuel density effect, while U-233 fission is the dominant contribution for JEFF-3.1.2 and ENDF/B-VII.1. Also the contribution of the inelastic scattering reaction in F-19 is large in JEFF-3.1.2 and ENDF/B.VII.1, while no covariance data is available in JENDL-4.0.

In further research, the following points must be addressed: first, the covariance data for Li-7, F-19, Th-232 and U-233 needs to be added and/or reviewed for consistency. The role of Li-7 and F-19 in the Doppler effect needs to be investigated. The inelastic scattering cross section and the associated distribution of the out-going energy of F-19 needs to be investigated.

In the present analysis, the uncertainty on the depletion behavior of the individual fuel isotopes has not been taken into account. In reality, the uncertainty of the isotopic depletion introduces an uncertainty on the composition of the fuel salt. The resulting uncertainty on the multiplication factor may in fact be larger than the 3% spread that has been observed in the present analysis. A follow-up study should take into account the uncertainty of depletion.
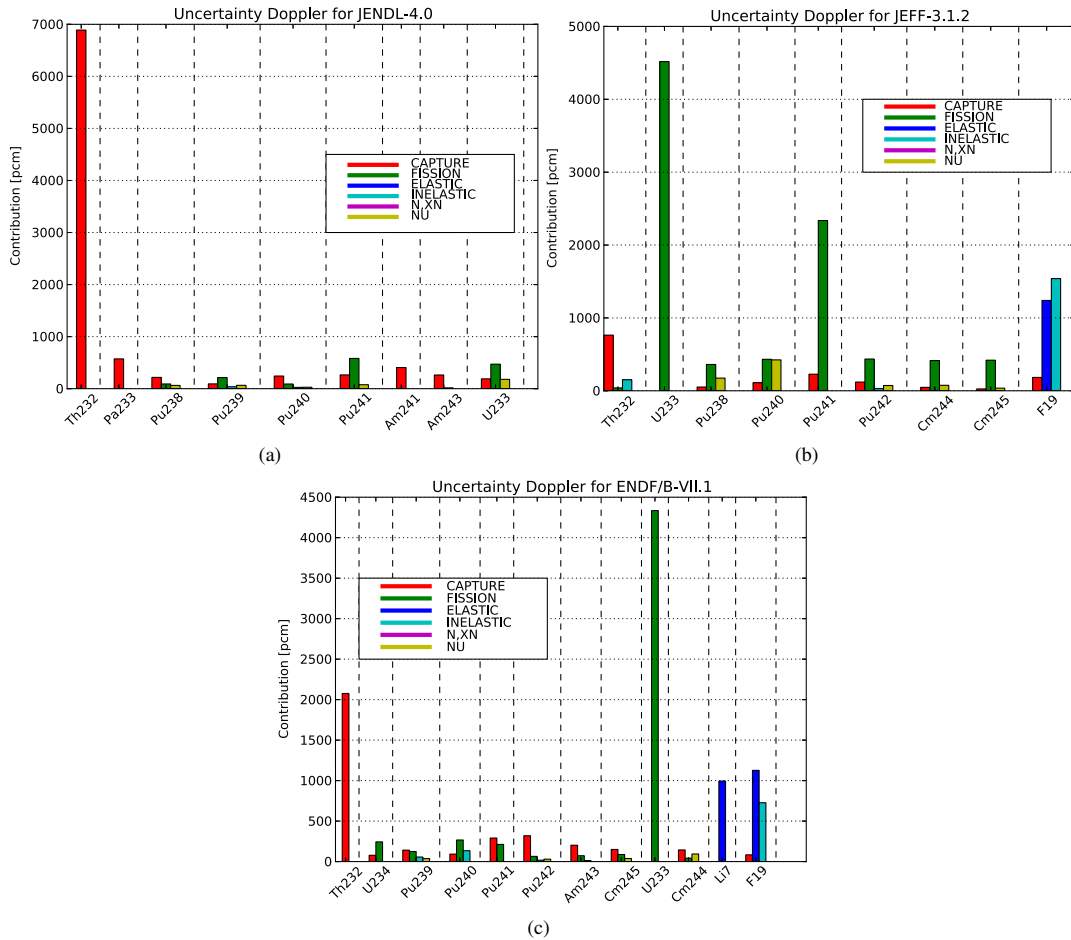
Fig. 8. For each set of nuclear data, the contribution of each isotope to the uncertainty of the Doppler coefficient.

References

[1] M.B. Seregin, A.P. Parshin, A.Yu. Kuznetsov, L.I. Ponomarev, S.A. Mel'nikov, A.A. Mikhalichenko, A.A. Rzheutskii, R.N. Manuilov, Solubility of UF_4, ThF_4, and CeF_3 in the $NaF-ZrF_4$ Melt, Radiochemistry 53 (1) (2011) 69 – 72, original Russian text piblished in Radiokhimiya, 2011, 53, 1, 63 - 65.
[2] M B. Seregin, A.P. Parshin, A.Yu. Kuznetsov, L.I. Ponomarev, S.A. Mel'nikova, A.A. Mikhalichenko, A.A. Rzheutskii, R.N. Manuilova, Solubility of UF_4, ThF_4, and CeF_3 in a $LiF-NaF-KF$ Melt, Radiochemistry 53 (5) (2011) 491 – 493, original Russion text published in Radiokhimiya, 2011, 53, 5, 416 - 418.
[3] O. Beneš, R.J.M. Konings, Thermodynamic assessment of the $LiF-CeF_3-ThF_4$ system: prediction of the PuF_3 concentration in a molten salt reactor fuel, Journal of Nuclear Materials 435 (2013) 164 – 171.
    URL http://dx.doi.org/10.1016/j.jnucmat.2012.12.005
[4] E. Capelli, O. Beneš, M. Beilmann, R.J.M. Konings, Thermodynamic investigation of the $LiF-ThF_4$ system, J. Chem. Thermo-dynamics 58 (2013) 110 – 116.
    URL http://dx.doi.org/10.1016/j.jct.2012.10.013
[5] Leslie C. Dewan, Christian Simon, Paul A. Madden, Linn W. Hobbs, Mathieu Salanne, Molecular dynamics simulation of the thermodynamic and transport properties of the molten salt fast reactor fuel $LiF-ThF_4$, Journal of Nuclear Materials 434 (2013) 322 – 327.
    URL http://dx.doi.org/10.1016/j.jnucmat.2012.12.006
[6] ORNL, SCALE: A Modular Code System for Performing Standardized Computer Analyses for Licensing Evaluation, Oak Ridge National Laboratory, ORNL/TM-2005/39, Version 6, Vols. I - III (Jan. 2009).
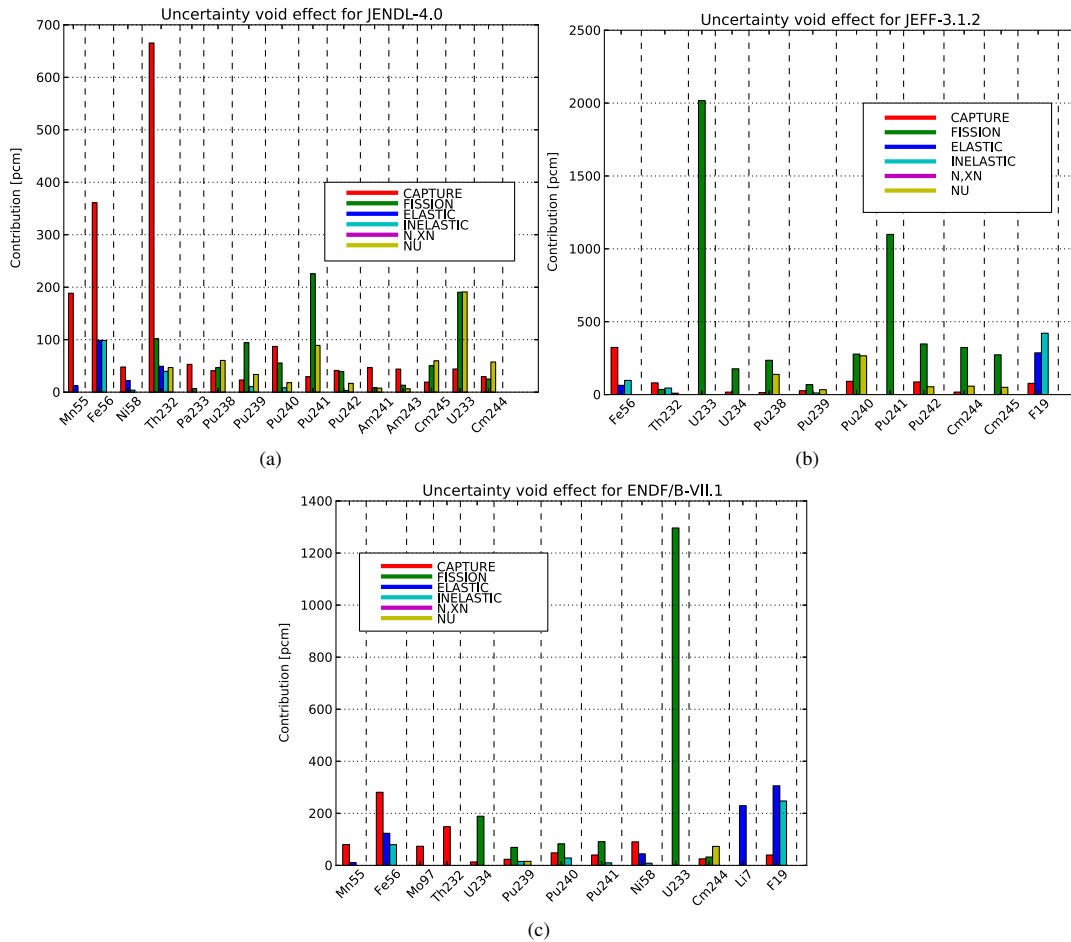
Fig. 9. For each set of nuclear data, the contribution of each isotope to the uncertainty of the fuel density coefficient.

[7] G. Rimpault, D. Plisson, J. Tommasi, R. Jacqmin, J.-M. Rieunier, D. Verrier, D. Biron, The ERANOS code and data system for fast reactor neutronic analyses, in: Physor 2002, ANS, Seoul, South Korea, 2002.

[8] W. van Rooijen, Analysis of the MZA/MZB benchmarks with modern nuclear data, Annals of Nuclear Energy 62 (2013) 504 - 525. doi:10.1016/j.anucene.2013.07.013.

[9] W. van Rooijen, N. Yamano, Analysis of the neutronic properties of the prototype FBR Monju based on several evaluated nuclear data libraries, in: ND2013, BNL, New York, NY, USA, 2013.

[10] Florian Jolivet, Analysis of the reactivity feedback coefficients of the prototype FBR Monju, Master's thesis, Institut National des Sciences et Techniques Nucléaires (INSTN) (Nov. 2012).

[11] M. Salvatores, R. Jacqmin, Uncertainty and target accuracy assessment for innovative systems using recent covariance data evaluations, Tech. Rep. NEA/WPEC-26, ISBN 978-92-64-99053-1, Argonne National Laboratory / CEA / OECD Nuclear Energy Agency (2008).
URL http://www.oecd-nea.org/science/wpec/volume26/volume26.pdf